

## A genetic-algorithm-based neural network approach for EDXRF analysis\*

WANG Jun (王俊),<sup>1</sup> LIU Ming-Zhe (刘明哲),<sup>1,†</sup> TUO Xian-Guo (庾先国),<sup>1,2</sup>LI Zhe (李哲),<sup>1</sup> LI Lei (李磊),<sup>1</sup> and SHI Rui (石睿)<sup>1</sup><sup>1</sup>State Key Laboratory of Geohazard Prevention and Geoenvironment

Protection (Chengdu University of Technology), Chengdu 610059, China

<sup>2</sup>Key Subject Laboratory of National Defense for Radioactive Waste and Environmental Security,  
Southwest University of Science and Technology, Mianyang 621010, China

(Received August 23, 2013; accepted in revised form May 17, 2014; published online June 20, 2014)

In energy dispersive X-ray fluorescence (EDXRF), quantitative elemental content analysis becomes difficult due to the existence of the noise, the spectrum peak superposition, element matrix effect, etc. In this paper, a hybrid approach of genetic algorithm (GA) and back propagation (BP) neural network is proposed without considering the complex relationship between the elemental content and peak intensity. The aim of GA-optimized BP is to get better network initial weights and thresholds. The starting point of this approach is that the reciprocal of the mean square error of the initialization BP neural network is set as the fitness value of the individuals in GA; and the initial weights and thresholds are replaced by individuals, then the optimal individual is searched by selecting, crossover and mutation operations, finally a new BP neural network model is established with the optimal initial weights and thresholds. The quantitative analysis results of titanium and iron contents in five types of mineral samples show that the relative errors of 76.7% samples are below 2%, compared to chemical analysis data, which demonstrates the effectiveness of the proposed method.

Keywords: EDXRF, Quantitative analysis, BP neural network, Genetic algorithm

DOI: [10.13538/j.1001-8042/nst.25.030203](https://doi.org/10.13538/j.1001-8042/nst.25.030203)

## I. INTRODUCTION

Vanadium-bearing titanomagnetite is an important source of iron and titanium oxide, with highly comprehensive utilization values. It is characterized by complex element composition, hence there is an essential need of elemental analysis to estimate mineral species in industries. Traditional chemical analysis is accurate but time consuming and costly. Energy dispersive X-ray fluorescence (EDXRF) is a non-destructive technique widely used in mining industry [1].

EDXRF-based instruments have been developed and commercialized for cement and mineral production, ore exploration, environmental monitoring, mine mapping, process monitoring, etc. [2–6]. While matrix effect is a key factor for accuracy of EDXRF analysis of complex samples, especially the absorption-enhancement effect among elements. This effect can greatly interfere the fluorescence counting rate and cause big errors between the counting rate and element content. Therefore, seeking appropriate method to correct the matrix effect and improve analysis accuracy is an important research issue in X-ray analysis [7–9]. To a large extent, traditional correction methods, either experimental or mathematical, depend on accuracy of standard samples [10]. The fundamental parameter (FP) methods are hindered by difficulties in obtaining accurate basic parameters [11]. Recently using Radial Basis Function (RBF) neural network to adjust the matrix effect has received good results as reported in Ref. [12].

In this paper, a hybrid algorithm of genetic algorithm (GA) and back propagation (BP) neural network is proposed without considering the complex relationship between the concentration and intensity. The aim of GA-optimizing BP is to get better network initial weights and thresholds. The basic idea is as follows: The reciprocal of the mean square error of the initialization BP neural network is set as the fitness value of the individual in GA; the initial weights and thresholds are replaced by individuals, the optimal individual is searched by selecting, crossover and mutation operations, and a new BP neural network model is finally established with the optimal initial weights and thresholds.

The outline of the paper is as follows. The model formation is conducted in Sec. II. In Sec. III, we discuss the computational results and the effectiveness of the proposed model. Finally, conclusions are given in Sec. IV.

## II. METHODOLOGY

The GA-BP model has three layers with  $m$  nodes in the input layer,  $h$  nodes in the hidden layer, and  $n$  nodes in the output layer. The model is implemented to determine a basic state space of connection weights matrix. Then, the number of hidden nodes and connection weights matrix are encoded into a mixed string that consists of integer value and real value [13, 14]. In this paper the experimental data is divided into two parts: training samples and testing samples. The scheme is described as follows:

Step 1: In the calculations, a three-layered BP neural network is employed to estimate basic state space of connection weights that are within  $[-1, 1]$  for the training samples.

Step 2: Encode connection weights and number of hidden nodes. The hidden nodes are encoded as binary code string:

\* Supported by National Outstanding Youth Science Foundation of China (No. 41025015), the National Natural Science Foundation of China (No. 41274109) and Sichuan Youth Science and Technology Innovation Research Team (No. 2011JTD0013)

† Corresponding author, [liumz@cdut.edu.cn](mailto:liumz@cdut.edu.cn)

1, ..., 1	0.2, ..., 0.7	0.3, ..., 0.1	0.2, ..., 0.3	0.9, ..., 0.8
<i>A</i>	<i>B</i>	<i>C</i>	<i>D</i>	<i>E</i>

1 is for connection to input and output nodes; and 0 with no connection. The weights are encoded as float string, with string length  $H = m * h + h + h * n + n$  ( $m$  is the number of input nodes,  $n$  is the number of output nodes,  $h$  is the number of hidden nodes). Each string corresponds to a chromosome, which consists of some gene sections, tabulated as above illustrations. Where, *A* stands for the number of hidden neurons; *B* stands for weights between input and hidden neurons; *C* stands for threshold of hidden neurons; *D* stands for weights between hidden and output neurons; *E* stands for threshold of output neurons. *A* is encoded in binary type, and other parts in real value. The values change in training period.

Step 3: Initialize a population of chromosomes. The length  $L$  of each chromosome equals to  $G + H$ , where  $G$  is the length of binary code of the hidden node numbers and  $H$  is the length of real-valued code of connection weights.

Step 4: Calculate fitness individually using Eq. (1),

$$f(x) = \frac{1}{SE} = \frac{1}{sse(T' - T)} = \frac{1}{\sum_{i=1}^n (t'_i - t_i)^2}, \quad (1)$$

where  $T' = \{t'_1, t'_2, \dots, t'_n\}$  is the desired output, and  $T = \{t_1, t_2, \dots, t_n\}$  is the real data.

Step 5: Calculate the sum of all fitness values of the individuals in a population, and calculate relative fitness value of each individual using Eq. (2), as the probability of heredity to the next generation. Then copy the highest fitness individual directly to a new offspring, and select other individuals by the method of spinning the roulette wheel [15].

$$F = \sum_{i=1}^n f(X_i), P_i = \frac{f(X_i)}{F}. \quad (2)$$

Step 6: Use basic crossover and mutation operations to the control code, namely, if a hidden node is deleted (added) according to mutation operation, the corresponding control code is encoded to be 0 (or 1). The crossover and mutation operators of weights are encoded as follows:

(a) Crossover operation with probability  $p_c$  (the subscript  $c$  denotes "crossover operation")

$$X_i^{t+1} = c_i X_i^t + (1 - c_i) X_{i+1}^t, \quad (3)$$

$$X_{i+1}^{t+1} = (1 - c_i) X_i^t + c_i X_{i+1}^t, \quad (4)$$

where  $X_i^t$  and  $X_{i+1}^t$  are a pair of individuals before crossover,  $X_i^{t+1}$  and  $X_{i+1}^{t+1}$  are a pair of individuals after crossover,  $c_i$  is taken as random value within [0,1].

(b) Mutation operation with probability  $p_m$  (the subscript  $m$  denotes "mutation operation")

$$X_i^{t+1} = X_i^t + c_i, \quad (5)$$

where  $X_i^t$  is individual before mutation,  $X_i^{t+1}$  is individual after mutation  $c_i$  is taken as random value within [0,1]

Step 7: Generate the new population and replace the current population. Steps 4~7 are repeated until convergence conditions are satisfied.

Step 8: Decode the highest fitness individual, obtain corresponding thresholds and connection weights, and use the new weights and thresholds to train network again. Then, output the prediction results.

### III. MODEL IMPLEMENTATION AND RESULTS

Mineral samples were collected in two mine plants in Panzhihua, Sichuan province, China, 40 sample groups from each plant. The samples included five mineral types: iron ore concentrate, iron gangues, titanium concentrates, titanium gangues and raw ore. Each sample group was about 4 kg. They were smashed and ground into powders in an agate mortar for 30 minutes, so as to ensure the homogeneity and reduce the granularity effect. The powders were sieved to 180 meshes and dried for 1 hour in an oven at 105 °C~110 °C in order to reduce the humidity effect. The samples for EDXRF measurement were prepared by tabulating the mineral powders.

The samples were analyzed by a typical EDXRF experiment setup, containing a vacuum chamber (to reduce the counts from argon in the air), an X-ray tube, a sample carrier and a detector. The X-ray tube was operated at 12.25 keV and 25.56 μA. Fluorescent X-rays from the samples were detected by an electric cooled Si(PIN) semiconductor detector with an energy resolution of 180 eV to 190 eV for 5.9 keV. Each group was measured for three times and each measurement lasts 3 minutes. The final spectrum was obtained by calculating the mean counting rate of the three measurements.

The five types of mineral samples contain 10 metal elements, i.e. Ca, V, Cr, Ni, Cu, Zn, As, Pb, Ti and Fe, with Fe and Ti being the main composition elements. The counting rates (per channel) in the spectrum section of 4.038 keV to 8.364 keV (280~580 channels after energy calibration) were chosen as main factor of element content influence. Elements in this section contains  $K\alpha$  X-ray peaks of Ti (4.510 keV), Fe (6.403 keV), V (4.951 keV), Ni (7.477 keV) and Cu (8.046 keV). So, the competition layer structure in GA-BP network is designed for  $9 \times 2$  dimensions, as there are 9 hidden nodes and 2 output neurons. The hidden nodes are obtained according to the empirical formula  $\log_2 n$ , where  $n$  is the number of neurons in input. The count rate in each channel was taken as the input vector of GA-BP net, and the Ti and Fe concentrations as GA-BP network output variables. The activation function adopted here from input to hidden layer is logsig, while from hidden to output layer it is purelin function, and the training function is traincgb. For the proposed hybrid neural network, the parameters in Table 1 were applied to training samples and prediction.

For the five types of minerals, we did 30 times of training and forecast, and calculated the average relative prediction error, standard deviation and coefficient of variation (CV), as a judgment standard of accuracy and precision of the model. In Table 2, for 76.7% of the samples, the GA-BP forecast

TABLE 1. Required model parameters

Name of Variables	Value	Name of Variables	Value
Training Sample	50	training function	traincgb()
Testing Sample	30	transfer function(H)	logsig()
Number of Input Nodes	301	transfer function(O)	purelin()
Number of Hidden Nodes	9	Crossover Probability $p_c$	0.80
Number of Output Nodes	2	Mutation Probability $p_m$	0.09
Learning Rate	0.05	Population	20
Training Epochs	1000	Generation Number	20
Training Goal (MSE)	$10^{-7}$		

TABLE 2. The experimental results averaging 30 times

Sample	Fe%					Ti%				
	Chemical analysis	GA-BP forecast	Relative% error%	Standard% deviation%	CV %	Chemical analysis	GA-BP forecast	Relative% error%	Standard% deviation%	CV %
Iron ore gangue	19.21	19.00	1.07	0.099	0.53	5.61	5.55	1.09	0.034	0.61
	18.83	18.95	0.60	0.098	0.52	5.50	5.54	0.56	0.030	0.54
	18.48	18.98	2.75	0.093	0.49	5.40	5.55	2.85	0.022	0.40
	19.21	19.04	0.88	0.094	0.49	5.61	5.56	0.93	0.028	0.50
	18.83	18.93	0.49	0.106	0.56	5.50	5.52	0.28	0.023	0.42
	18.48	18.73	1.39	0.103	0.55	5.40	5.48	1.49	0.021	0.39
Concentrated titanium ore	35.05	34.63	1.18	0.18	0.51	27.28	26.97	1.14	0.14	0.53
	34.36	34.28	0.24	0.11	0.32	26.75	26.71	0.16	0.08	0.31
	33.71	34.75	3.08	0.17	0.50	26.24	27.08	3.17	0.13	0.47
	35.04	34.88	0.48	0.16	0.45	27.28	27.13	0.58	0.11	0.41
	34.37	34.82	1.31	0.15	0.44	26.76	27.07	1.19	0.10	0.37
	33.71	34.67	2.84	0.13	0.36	26.24	26.98	2.79	0.11	0.42
Titanium ore gangue	14.85	14.75	0.67	0.065	0.44	3.32	3.29	0.73	0.015	0.44
	14.56	14.67	0.71	0.078	0.53	3.25	3.27	0.77	0.016	0.50
	14.28	14.69	2.83	0.11	0.77	3.19	3.27	2.60	0.027	0.83
	14.85	14.68	1.14	0.067	0.47	3.31	3.28	1.06	0.019	0.56
	14.56	14.72	1.05	0.075	0.51	3.25	3.28	0.97	0.014	0.43
	14.29	14.60	2.33	0.084	0.57	3.19	3.26	2.18	0.022	0.66
Concentrated iron ore	54.45	53.91	0.99	0.28	0.52	7.70	7.62	1.08	0.037	0.48
	53.40	53.92	0.97	0.22	0.40	7.55	7.63	1.00	0.036	0.47
	52.37	53.56	2.46	0.23	0.43	7.41	7.58	2.28	0.030	0.40
	54.44	53.71	1.35	0.34	0.63	7.70	7.59	1.47	0.042	0.55
	53.39	53.17	0.42	0.30	0.57	7.55	7.52	0.43	0.034	0.45
	52.38	53.40	1.99	0.26	0.48	7.41	7.55	1.93	0.032	0.43
Original mine	31.78	31.43	1.15	0.13	0.44	6.51	6.45	0.97	0.028	0.44
	31.16	31.24	0.26	0.17	0.53	6.39	6.41	0.30	0.030	0.47
	30.57	31.26	2.25	0.24	0.46	6.27	6.41	2.31	0.035	0.54
	31.78	31.62	0.59	0.20	0.65	6.51	6.48	0.52	0.028	0.42
	31.16	31.27	0.68	0.18	0.58	6.39	6.41	0.43	0.034	0.52
	30.57	31.09	1.83	0.18	0.59	6.27	6.37	1.67	0.048	0.75

results of Ti and Fe contents in the five types of minerals are almost the same as the chemical analysis results (with relative errors of less than 2%). Table 3 and Fig. 1 show the whole genetic process and the convergence of the genetic algorithm. It is found that the model shows a fast convergence and high efficient fitness process.

TABLE 3. Epochs and fitness value

Value	Epochs	Fitness
Min	21	0.0537
Max	74	0.1034
Average	38	0.0719

IV. CONCLUSION

For accurate analysis of EDXRF, new techniques for data processing against the effect of absorption-enhancement among elements are of importance. Based on previous stud-

ies, we proposed a hybrid GA-BP approach for data handling of EDXRF spectra of complex samples, such as vanadium-bearing titanomagnetite. The established GA-BP model has features of memorizing new type, associating existed type, studying unknown type, and finally achieving effective pre-

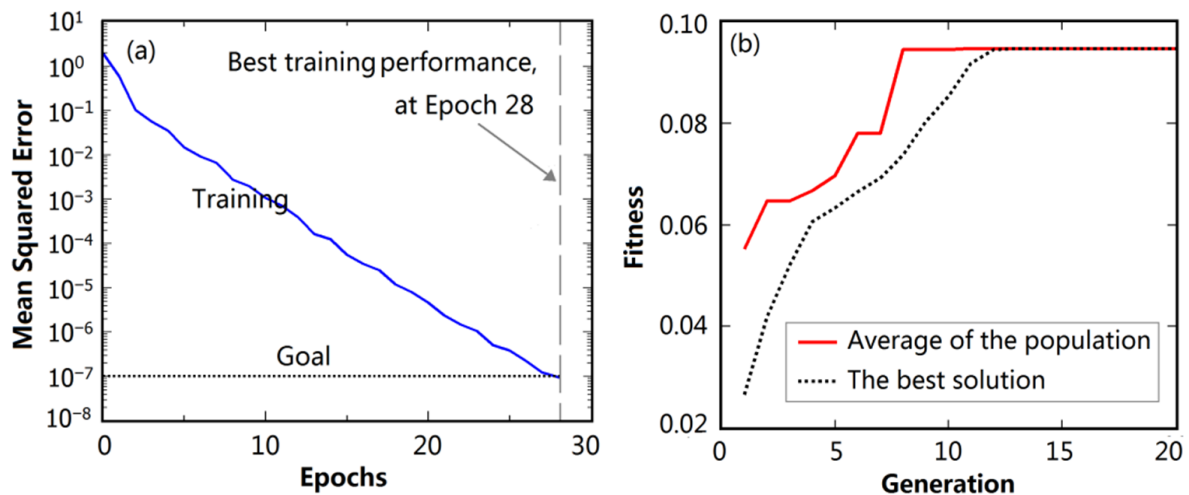


Fig. 1. (a) Best training performance and (b) fitness function of concentrated titanium ore.

diction of complex samples. By doing so, the model can reduce matrix effect and improve measurement results of complex samples. In the future work, we would like to col-

lect more ore samples in Panzhihua field to test the model effectiveness and judge the generalization ability of the proposed model for all available samples in Panzhihua field.

- 
- [1] Li Z, Tuo X G, Yang J B, *et al.* Nucl Sci Tech, 2012, **23**: 289–294.
  - [2] Frangi J P and Richard D. Sci Total Environ, 1997, **205**: 71–79.
  - [3] Sumpun W, Phadoong B, Thippawan S. Hydrometallurgy, 1997, **45** : 161–167.
  - [4] Orhan M K, Zafer U, Iknur O, *et al.* J Quant Spectrosc Ra, 2007, **103**: 424–427.
  - [5] GonzalezFern O, Queralt I, Carvalho M L, *et al.* Nucl Instrum Meth B, 2007, **262**: 81–86.
  - [6] Natarajan V, Porwal N K, Babu Y, *et al.* Appl Radiat Isotopes, 2010, **68**: 1128–1131.
  - [7] Richard M. Rousseau. Spectrochim Acta B, 2006, **61**: 759–777.
  - [8] Sherman J. Spectrochim Acta, 1955, **7**: 283–306.
  - [9] Lachance G R and Traill R J. Can Spectrosc, 1966, **11**: 43–48.
  - [10] Cao L G. Nucl Tech, 1987, **10**: 15–21. (in Chinese)
  - [11] Cao L G, Ding Y M, Huang Z Q. Method of Energy Dispersive X-ray Fluorescence. Chengdu: Chengdu University of Science and Technology Press, 1998, 182–274.
  - [12] Li Z, Tuo X G, Mu K L. Nucl Sci Tech, 2009, **32**: 35–40.
  - [13] Kima G H, Yoona J E, An S H, *et al.* Build Environ, 2004, **39**: 1333–1340.
  - [14] Ozkaya B, Demi A, Bilgili M S. Environ Modeling Software, 2007, **22**: 815–822.
  - [15] Messai N, Thomas P, Lefebvre D, *et al.* A neural Network Approach for freeway Traffic Flow Prediction. In Proceedings of the 2002 IEEE International Conference on Control Applications, Glasgow, Scotland, U.K, September 2002, 18–20.